

Genomics of Mesolithic Scandinavia reveal colonization routes and high-latitude adaptation

Torsten Günther^{1,*†}, Helena Malmström^{1,*}, Emma M. Svensson^{1,*}, Ayça Omrak^{2,*}, Federico Sánchez-Quinto¹, Gülşah M. Kılınç^{1,2,3}, Maja Krzewińska², Gunilla Eriksson², Magdalena Fraser^{1,4}, Hanna Edlund¹, Arielle R. Munters¹, Alexandra Coutinho¹, Luciana G. Simões¹, Mário Vicente¹, Anders Sjölander¹, Berit Jansen Sellevold⁵, Roger Jørgensen⁶, Peter Claes⁷, Mark D. Shriver⁸, Cristina Valdiosera⁹, Mihai G. Netea¹⁰, Jan Apel¹¹, Kerstin Lidén^{2,6}, Birgitte Skar¹², Jan Stora^{2,†}, Anders Götherström^{2,13†}, Mattias Jakobsson^{1,13,†}

* These authors contributed equally.

¹ Department of Organismal Biology, Uppsala University, Norbyvägen 18C, 75236, Uppsala, Sweden

² Department of Archaeology and Classical Studies, Stockholm University, Wallenberglaboratoriet, 10691 Stockholm, Sweden

³ Middle East Technical University, Department of Biological Sciences, 06800, Ankara, Turkey

⁴ Department of Archaeology and Ancient History, Uppsala University-Campus Gotland, 62167 Visby, Sweden

⁵ NIKU - Norwegian Institute for Cultural Heritage Research

⁶ Tromsø University Museum, UiT The Arctic University of Norway, P.O. Box 6050 Langnes, NO-9037 Tromsø, Norway

⁷ Department of Electrical Engineering, ESAT/PSI, KU Leuven, 3000, Leuven, Belgium

⁸ Department of Anthropology, Penn State University, 16801, University Park, USA

⁹ Department of Archaeology and History, La Trobe University, Melbourne, VIC 3086, Australia

¹⁰ Department of Internal Medicine and Radboud Center for Infectious Diseases, Radboud University Medical Center, Geert Grooteplein 8, 6525GA Nijmegen, The Netherlands

¹¹ Department of Archaeology and Ancient History, Lund University, 22100, Lund, Sweden

¹² Department of Archaeology and Cultural History, NTNU University Museum, 7491 Trondheim, Norway

¹³ SciLife Lab

† Corresponding authors

29 **Abstract**

30 Scandinavia was one of the last geographic areas in Europe to become habitable for humans after
 31 the last glaciation. However, the origin(s) of the first colonizers and their migration routes remain
 32 unclear. We sequenced the genomes, up to 57x coverage, of seven hunter-gatherers excavated
 33 across Scandinavia and dated to 9,500-6,000 years before present. Surprisingly, among the
 34 Scandinavian Mesolithic individuals, the genetic data display an east-west genetic gradient that
 35 opposes the pattern seen in other parts of Mesolithic Europe. This result suggests that
 36 Scandinavia was initially colonized following two different routes: one from the south, the other
 37 from the northeast. The latter followed the ice-free Norwegian north Atlantic coast, along which
 38 novel and advanced pressure-blade stone-tool techniques may have spread. These two groups met
 39 and mixed in Scandinavia, creating a genetically diverse population, which shows patterns of
 40 genetic adaptation to high latitude environments. These adaptations include high frequencies of
 41 low pigmentation variants and a gene-region associated with physical performance, which shows
 42 strong continuity into modern-day northern Europeans.

43 Introduction

44 As the ice-sheet retracted from northern Europe after the Last Glacial Maximum (LGM), around
 45 23,000 years ago, new habitable areas emerged [1] allowing plants [2,3] and animals [4,5] to
 46 recolonize the Scandinavian peninsula (hereafter Scandinavia). There is consistent evidence of
 47 human presence in the archaeological record from c. 11,700 years before present (BP), both in
 48 southern and northern Scandinavia [6–9]. At this time, the ice-sheet was still dominating the
 49 interior of Scandinavia [9] (Fig. 1A, S1 Text), but recent climate modeling shows that the Arctic
 50 coast of (modern-day) northern Norway was ice-free [10]. Similarities in late-glacial lithic
 51 technology (direct blade percussion technique) of western Europe and the oldest counterparts of
 52 northernmost Scandinavia [11] (S1 Text) have been used to argue for a postglacial colonization of
 53 Scandinavia from southwestern Europe. However, studies of a new lithic technology, ‘pressure
 54 blade’ technique, which first occurred in the northern parts of Scandinavia, indicates contacts
 55 with groups in the east and possibly an eastern origin of the colonizers [7,12,13] (S1 Text). The
 56 first genetic studies of Mesolithic human remains from central and eastern Scandinavia (SHGs)
 57 revealed similarities to two different Mesolithic European populations, the ‘western hunter-
 58 gatherers’ (WHGs) from western, central and southern Europe and the ‘eastern hunter-gatherers’
 59 (EHGs) from northeastern Europe [14–21]. Archaeology, climate modeling, and genetics, suggest
 60 several possibilities for the colonization of Scandinavia, including migrations from the south,
 61 southeast, northeast and combinations of these, however, the early post-glacial peopling of
 62 Scandinavia remains elusive [1,4,6–17,22,23]. In this study, we contrast genome sequence data
 63 and stable isotopes from Mesolithic human remains from western, northern, and eastern
 64 Scandinavia to infer the post-glacial colonization of Scandinavia – from where people came,

65 what routes they followed, how they were related to other Mesolithic Europeans [15–19,24] –
66 and to investigate human adaptation to high-latitude environments.

67 **Results and Discussion**

68 We sequenced the genomes of seven hunter-gatherers from Scandinavia (Table 1; S1 Text, S2
69 Text, S3 Text) ranging from 57.8× to 0.1× genome coverage, of which four individuals had a
70 genome coverage above 1×. The remains were directly dated to between 9,500 BP and 6,000 BP,
71 and were excavated in southwestern Norway (Hum1, Hum2), northern Norway (Steigen), and the
72 Baltic islands of Stora Karlsö and Gotland (SF9, SF11, SF12 and SBj) and represent 18% (6 of
73 33) of all known human remains in Scandinavia older than 8,000 [25]. All samples displayed
74 fragmentation and cytosine deamination at fragment termini characteristic for ancient DNA (S3
75 Text). Mitochondrial (mt) DNA-based contamination estimates were <6% for all individuals and
76 autosomal contamination was <1% for all individuals except for SF11, which showed c. 10%
77 contamination (Table 1, S4 Text). Four of the seven individuals were inferred to be males, three
78 were females. All the western and northern Scandinavian individuals and one eastern
79 Scandinavian carried U5a1 mitochondrial haplotypes while the remaining eastern Scandinavians
80 carried U4a haplotypes (Table 1, S5 Text). These individuals represent the oldest U5a1 and U4
81 lineages detected so far. The Y chromosomal haplotype was determined for three of the four
82 males, all carried I2 haplotypes, which were common in pre-Neolithic Europe (Table 1, S5 Text).

Table 1: Information on the seven Scandinavian hunter-gatherers investigated in this study, including calibrated date before present (cal BP) corrected for the marine reservoir effect, given as a range of two standard deviations, average genome coverage, average mitochondrial (mt) coverage, mt and Y chromosome haplogroups and contamination estimates based on the mt, the X-chromosome for males and the autosomes.

Individual	Calibrated date (cal BP, 2 sigma)	Genome coverage	mt coverage	Sex	mt haplo-group	Y haplo-group	Contamination estimate		
							based on mt	based on X	based on autosomes
Hum1	9452-9275 ^s	0.71	597	XX	U5a1	-	0.29%	-	0.00%
Hum2	9452-9275 ^s	4.05	432	XY	U5a1d	I2-L68	0.15%	0.63%	0.73%
Steigen	5950-5764	1.24	277	XY	U5a1d	I2a1b-M423	0.00%	0.4%	0.00%
SF9	9300-8988	1.15	93	XX	U4a2	-	5.36%	-	0.00%
SF11	9023-8760	0.10	45	XY	U5a1	*	3.42%	*	10.16%
SF12	9033-8757	57.79	9774	XX	U4a1	-	0.34%	-	0.932%
SBj	8963-8579	0.43	102	XY	U4a1	I2-L68	3.72%	1.4%	0.06%

^s combined probability for the Hummervikholmen samples

* not enough genome coverage

90

91

The high coverage and Uracil-DNA-glycosylase (UDG) treated genome (to reduce the effects of

post-mortem DNA damage [26]) of SF12 allowed us to confidently discover new and hitherto

unknown variants at sites with 55x or higher sequencing depth (S3 Text). Based on SF12's high-

coverage and high-quality genome, we estimate the number of single nucleotide polymorphisms

(SNPs) hitherto unknown (that are not recorded in dbSNP (v142)) to be c. 10,600. This is almost

twice the number of unique variants (c. 6,000) per Finnish individual (S3 Text) and close to the

median per European individual in the 1000 Genomes Project [27] (c. 11,400, S3 Text). At least

17% of these SNPs that are not found in modern-day individuals, were in fact common among

the Mesolithic Scandinavians (seen in the low coverage data conditional on the observation in

SF12), suggesting that a substantial fraction of human variation has been lost in the past 9,000

years (S3 Text). In other words, the SHGs (as well as WHGs and EHG) have no direct

descendants, or a population that show direct continuity with the Mesolithic populations [14–17].

Thus, many genetic variants found in Mesolithic individuals have not been carried over to

102 modern-day groups. Among the novel variants in SF12, four (all heterozygous) are predicted to
 103 affect the function of protein coding genes [28] (S3 Text). The ‘heat shock protein’ *HSPA2* in
 104 SF12 carries an unknown mutation that changes the amino acid histidine to tyrosine at a protein-
 105 protein interaction site, which likely disrupts the function of the protein (S3 Text). Defects in
 106 *HSPA2* are known to drastically reduce fertility in males [29]. Although SF12 herself would not
 107 be affected by this variant, her male offspring could carry the reduced fertility variant, and it will
 108 be interesting to see how common this variant was among Mesolithic groups as more genome
 109 sequence data become available. The high-quality diploid genotype calls further allowed us to
 110 genetically predict physical appearance, including pigmentation, and to use a model-based
 111 approach trained on modern-day faces and genotypes [30,31] to create a 3D model of SF12’s face
 112 (S9 Text). This represents a new way of reconstructing an ancient individual’s facial appearance
 113 from genetic information, which is especially informative in cases such as for SF12, where only
 114 post-cranial fragments were available, and future archaeogenetic studies will have the potential to
 115 many individuals appearance from past times.

116 *Demographic history of Mesolithic Scandinavians*

117 In order to compare the genomic data of the seven SHGs to genetic information from other
 118 ancient individuals and modern-day groups, data was merged with six published Mesolithic
 119 individuals from Motala in central Scandinavia, 47 published Upper Paleolithic, Mesolithic and
 120 Early Neolithic individuals from other parts of Eurasia (S6 Text) [15–20,24,32–36], as well as
 121 with a world-wide set of 203 modern-day populations [16,27,37]. All 13 SHGs – regardless of
 122 geographic sampling location and age – display genetic affinities to both WHGs and EHG (Fig.
 123 1A, B, S6 Text). This is consistent with a scenario in which SHGs represent a mixed group
 124 tracing parts of their ancestry to both the WHGs and the EHG [15–17,20,38].

125 To investigate the postglacial colonization of Scandinavia, we explored four hypothetical
 126 migration routes (primarily based on natural geography) linked to WHGs and EHG, respectively
 127 (S11 Text); a) a migration of WHGs from the south, b) a migration of EHG from the east across
 128 the Baltic Sea, c) a migration of EHG from the east and along the north-Atlantic coast, d) a
 129 migration of EHG from the east and south of the Baltic Sea, and combinations of these four
 130 migration routes. These scenarios allow us to formulate expected genetic affinities for northern,
 131 western, eastern, and central SHGs (S11 Text). The SHGs from northern and western Scandinavia
 132 show a distinct and significantly stronger affinity to the EHG compared to the central and
 133 eastern SHGs (Fig. 1). Conversely, the SHGs from eastern and central Scandinavia were
 134 genetically more similar to WHGs compared to the northern and western SHGs (Fig. 1). Using
 135 [16,17], the EHG genetic component of northern and western SHGs was estimated to 55% on
 136 average (43-67%) and significantly different (Wilcoxon test, $p=0.014$) from the average 35% (22-
 137 44%) in eastern and south-central SHGs. This average is similar to eastern Baltic hunter-gatherers
 138 from Latvia [33] (average 33%, Fig. 1A, S6 Text). These patterns of genetic affinity within SHGs
 139 are in direct contrast to the expectation based on geographic proximity with EHG and WHGs
 140 and do not correlate with age of the sample (S11 Text).

141 The archaeological record in Scandinavia shows early evidence of human presence in northern
 142 coastal Atlantic areas [13]. Stable isotope analysis of northern and western SHGs revealed an
 143 extreme marine diet, suggesting a maritime subsistence, in contrast to the more mixed
 144 terrestrial/aquatic diet of eastern and central SHGs (S1 Text). Combining these isotopic results
 145 with the patterns of genetic variation, we suggest an initial colonization from the south, likely by
 146 WHGs. A second migration of people who were related to the EHG – that brought the new
 147 pressure blade technique to Scandinavia and that utilized the rich Atlantic coastal marine

148 resources –entered from the northeast moving southwards along the ice-free Atlantic coast where
149 they encountered WHG groups. The admixture between the two colonizing groups created the
150 observed pattern of a substantial EHG component in the northern and the western SHGs, contrary
151 to the higher levels of WHG genetic component in eastern and central SHGs (Fig. 1, S11 Text).

152 By sequencing complete ancient genomes, we can compute unbiased estimates of genetic
153 diversity, which are informative of past population sizes and population history. Here, we restrict
154 the analysis to WHGs and SHGs, since only SNP capture data is available for EHG (S7 Text). In
155 current-day Europe, there is greater genetic diversity in the south compared to the north. During
156 the Mesolithic, by contrast, we find higher levels of genetic diversity (S7 Text) as well as lower
157 levels of runs of homozygosity (Fig. 2A) and linkage disequilibrium (Fig. 2B) in SHGs compared
158 to WHGs (represented by Loschbour and Bichon, [16,32]) and Caucasus hunter-gatherers (CHG,
159 represented by Kotias and Satsurblia, [32]). Using a sequential-Markovian-coalescent approach
160 [39] for the high-coverage, high quality genome of SF12, we find that right before the SF12
161 individual lived, the effective population size of SHGs was similar to that of WHGs (Fig. 2C). At
162 the time of the LGM and back to c. 50,000 years ago, both the WHGs and SHGs go through a
163 bottleneck, but the ancestors of SHGs retained a greater population size in contrast to the
164 ancestors of WHGs who went through a more severe bottleneck (Fig. 2C). Around 50,000-70,000
165 years ago, the effective population sizes of the ancestors of SHGs, WHGs, Neolithic groups
166 (represented by Stuttgart [16]) and Paleolithic Eurasians (represented by Ust-Ishim [36]) align,
167 suggesting that these diverse groups all trace their ancestry back to a common ancestral group
168 which likely represents the early migrants out-of-Africa, who likely share a common ancestry
169 outside of Africa.

170

171 *Adaptation to high-latitude environments*

172 With the aim of detecting signs of adaptation to high-latitude environments and selection during
 173 and after the Mesolithic, we employed three different approaches that utilize the Mesolithic
 174 genomic data. In the first approach, we assumed that SHGs adapted to high-latitude environments
 175 of low temperatures and seasonally low levels of light, and searched for gene variants that carried
 176 over to modern-day people in northern Europe. As we have already noted, modern-day northern
 177 Europeans trace limited amount of genetic material back to the SHGs (due to the many additional
 178 migrations during later periods), and any genomic region that displays extraordinary genetic
 179 continuity would be a strong candidate for adaptation in people living in northern Europe across
 180 time. We designed a statistic, D_{sel} (S10 Text), that captures this specific signal and scanned the
 181 whole genome for gene-variants that show strong continuity (little differentiation) between SHGs
 182 and modern-day northern Europeans while exhibiting large differentiation to modern-day
 183 southern European populations [40] (Fig. 3A; S10 Text). Six of the top ten SNPs with greatest
 184 D_{sel} values were located in the *TMEM131* gene that has been found to be associated with physical
 185 performance [41], which could make it part of the physiological adaptation to cold [42]. This
 186 genomic region was more than 200kbp long and showed the strongest haplotypic differentiation
 187 between modern-day Tuscans and Finns (S10 Text). The particular haplotype was relatively
 188 common in SHGs, it is even more common among today's Finnish population (S10 Text), and
 189 showed a strong signal of local adaptation (S10 Text). Other top hits included genes associated
 190 with a wide range of metabolic, cardiovascular, developmental and psychological traits (S10
 191 Text) potentially linked to physiological [42].

192 In addition to performing this genome-wide scan, we studied the allele frequencies in three
 193 pigmentation genes (*SLC24A5*, *SLC45A2*, having a strong effect on skin pigmentation, and

194 *OCA2/HERC2*, having a strong effect on eye pigmentation) where the derived alleles are virtually
 195 fixed in northern Europeans today. The differences in allele frequencies of those three loci are
 196 among the highest between human populations, suggesting that selection was driving the
 197 differences in eye color, skin and hair pigmentation as part of the adaptation to different
 198 environments [43–46]. The SHGs show a combination of eye and skin pigmentation that was
 199 unique in Mesolithic Europe, with light skin pigmentation and varied blue to light-brown eye
 200 color. This is strikingly different from the WHGs – who have been found to have the specific
 201 combination of blue-eyes and dark-skin [16,18,19,21] (Fig. 3B) – and EHG – who have been
 202 suggested to be brown eyed and light-skinned [17,18] (Fig. 3B). The unique configuration of the
 203 SHGs is not fully explained by the fact that SHGs are a mixture of EHG and WHGs as the
 204 frequencies of the blue-eye and one light-skin variant are significantly higher in SHGs than
 205 expected from their genome-wide admixture proportions (Fig. 3B, S10 Text). This could be
 206 explained by a continued increase of the allele frequencies after the admixture event, likely
 207 caused by adaptation to high-latitude environments [43,45].

208

209 **Conclusion**

210 By combining information from climate modeling, archaeology and Mesolithic human genomes,
 211 we were able to reveal the complexity of the early colonization process of Scandinavia and
 212 human adaptation to high-latitude environments. We disentangled migration routes and linked
 213 them to particular archaeological patterns, demonstrate greater genetic diversity in northern
 214 Europe compared to southern Europe – in contrast to modern-day patterns – and show that many
 215 genetic variants that were common in the Mesolithic have been lost today. These finds reiterate

the importance of human migration for dispersal of novel technology in human prehistory [14–17,23,24,38,47–50] and the many partial population turnovers in our past.

Materials and Methods

Sample preparation

Genomic sequence data was generated from teeth and bone samples belonging to seven (eight, including SF13) Mesolithic Scandinavian hunter-gatherers (S1 Text). A detailed description on the archaeological background of the samples as well as post-LGM Scandinavia can be found in S1 Text. Additional libraries were sequenced for Ajvide58 and Ajvide70 [15] (S2 Text). All samples were prepared in dedicated ancient DNA (aDNA) facilities at the Evolutionary Biology Centre in Uppsala (SF9, SF11, SF12, SF13, SBj, Hum1, Hum2) and at the Archaeological research laboratory, Stockholm University (Steigen).

DNA extraction and library building: Bones and teeth were decontaminated prior to analysis by wiping them with a 1% Sodiumhypoclorite solution, and DNA free water. Further, all surfaces were UV irradiated (6 J/cm² at 254 nm). After removing one millimeter of the surface, approximately 30-100 mg of bone was powderized and DNA was extracted following silica-based methods as in [51] with modifications as in [49,52] or as in [53] and eluted in 25-110 µl of EB buffer. Between one and 16 extractions were made from each sample and one extraction blank with water instead of bone powder was included per six to ten extracts. Blanks were carried along the whole process until qPCR and/or PCR and subsequent quantification.

237 DNA libraries were prepared using 20µl of extract, with blunt-end ligation coupled with P5 and
 238 P7 adapters and indexes as described in [49,54]. From each extract one to five double stranded
 239 libraries were built. Since aDNA is already fragmented the shearing step was omitted from the
 240 protocol. Library blank controls including water as well as extraction blanks were carried along
 241 during every step of library preparation. In order to determine the optimal number of PCR cycles
 242 for library amplification qPCR was performed. Each reaction was prepared in a total volume of
 243 25 µl, containing 1 ul of DNA library, 1X MaximaSYBRGreen mastermix and 200 nM each of
 244 IS7 and IS8 [54] reactions were set up in duplicates. Each blunt-end library was amplified in four
 245 to 12 replicates with one negative PCR control per index-PCR. The amplification reactions had a
 246 total volume of 25 µl, with 3 ul DNA library, and the following in final concentrations; 1X
 247 AmpliTaq Gold Buffer, 2.5mM MgCl₂, 250uM of each dNTP, 2.5U AmpliTaq Gold
 248 (Thermofisher), and 200nM each of the IS4 primer and index primer [54]. PCR was done with
 249 the following conditions; an activation step at 94°C for 10 min followed by 10-16 cycles of 94°C
 250 for 30s, 60°C for 30s and 72°C for 30s, and a final elongation step of 72°C for 10min. For each
 251 library four amplifications with the same indexing primer were pooled and purified with AMPure
 252 XP beads (Agencourt). The quality and quantity of libraries was checked using TapeStation or
 253 BioAnalyzer using the High Sensitivity Kit (Agilent Technologies). None of the blanks showed
 254 any presence of DNA comparable to that of a sample and were therefore not further analyzed. For
 255 initial screening 10-20 libraries were pooled at equimolar concentrations for sequencing on an
 256 Illumina HiSeq 2500 using v.4 chemistry and 125 bp paired-end reads or HiSeqX, 150bp paired-
 257 end length using v2.5 chemistry at the SNP & SEQ Technology Platform at Uppsala University.
 258 After evaluation of factors such as clonality, proportion of human DNA and genomic coverage

259 samples were selected for re-sequencing aiming to yield as high coverage as possible for each
260 library.

261

262 *Generation of a high coverage UDG treated genome:* Based on the results of the non-damage
263 repair sequencing the SF12 individual was selected for large-scale sequencing in order to
264 generate a high coverage genome of high quality where damages had been repaired using Uracil-
265 DNA-glycosylase (UDG). In addition to the 15 extracts previously prepared and used for non-
266 damage repair libraries, another 111 extracts were made based on a variety of silica based
267 methods [24,49,51,52]. From these 126 extracts a total of 258 damage repaired double stranded
268 libraries were built for Illumina sequencing platforms. Libraries were built as above, except a
269 DNA repair step with (UDG and endonuclease VIII (endo VIII) or USER enzyme (NEB)
270 treatment was included in order to remove deaminated cytosines [55]. Quantitative PCR (qPCR)
271 was performed in order to quantify the number of molecules and the optimal number of PCR
272 cycles prior to amplification for each DNA library. Furthermore, this step included extraction
273 blanks, library blanks and amplification blanks to monitor potential contamination. All of these
274 negative controls showed an optimal cycle of amplification significantly higher to those of our
275 ancient DNA libraries (>10 cycles) and they were thus deemed as negative. Our experimental
276 results show minimal levels of contamination, which is in concordance with mitochondrial DNA
277 and X chromosome estimates of contamination (see S4 Text and Table 1). Each reaction was
278 done in a total volume of 25 µl, containing 1 ul of DNA library, 1X MaximaSYBRGreen
279 mastermix and 200nM each of IS7 and IS8 [54] reactions were set up in duplicate. The PCRs
280 were set up using a similar system as for the non-damage repair samples (in quadruplicates that
281 were pooled when the PCR products were cleaned), with the difference of using AccuPrime DNA

282 polymerase instead of AmpliTaqGold (Thermofisher) and the following PCR conditions; an
 283 activation step at 95°C for 2 min followed by 10-16 cycles of 95°C for 15s, 60°C for 30s and
 284 68°C for 1min, and a final elongation step of 68°C for 5min. Blank controls including water as
 285 well as extraction blanks were carried out during every step of library preparation. Amplified
 286 libraries were pooled, cleaned, quantified and sequenced in the same manner as non-damage
 287 repaired libraries. In order to sequence libraries to depletion, two to eight libraries were pooled
 288 together and sequenced until reaching a clonality of >50%, if the clonality was lower, the library
 289 was either classified as unproductive or when the sequencing goal (>55X coverage) was reached
 290 and further sequencing was deemed unnecessary. Sequencing was performed as above.

291

292 *Bioinformatic data processing and authentication*

293 Paired-end reads were merged using MergeReadsFastQ_cc.py [56], if an overlap of at least 11
 294 base pairs was found the base qualities were added together and any remaining adapters were
 295 trimmed. Merged reads were then mapped single ended with bwa aln 0.7.13 [57] to the human
 296 reference genome (build 36 and 37) using the following non-default parameters: seeds disabled -l
 297 16500 -n 0.01 -o 2 [15,16]. To remove PCR duplicates, reads with identical start and end
 298 positions were collapsed using a modified version, to ensure random choice of bases, of
 299 FilterUniqSAMCons_cc.py [56]. Reads with less than 10 % mismatches to the human reference
 300 genome, reads longer than 35 base pairs and reads with mapping quality higher than 30 were used
 301 to estimate contamination.

302 The genetic data obtained from the two bone elements SF9 and SF13 showed extremely high
 303 similarities, which suggested that the two individuals were related. Using READ [58], a tool to

304 estimate kin-relationship from ancient DNA, SF9 and SF13 were classified as either identical
305 twins or the same individual. Therefore, we merged the genetic data for both individuals and refer
306 to the merged individual as SF9 throughout the genetic analysis.

307 All data shows damage patterns indicative of authentic ancient DNA (S3 Text). Contamination
308 was estimated using three different sources of data: (I) the mitochondrial genome [59], (II) the X
309 chromosome if the individual was male [60,61] and (III) the autosomes[62]. Low contamination
310 estimations over the three different approximations were interpreted as data mapping to the
311 human genome being largely endogenous (S4 Text).

312

313 *Analysis of demographic history*

314 Most population genomic analyses require a set of reference data for comparison. We compiled
315 three different data sets from the literature and merged them with the data from ancient
316 individuals (S6 Text). The three reference SNP panels were:

317

- 318 • The Human Origins genotype data set of 594,924 SNPs genotyped in 2,404 modern
319 individuals from 203 populations [16,37].
- 320 • A panel of 1,055,209 autosomal SNPs which were captured in a set of ancient individuals
321 by Mathieson et al [18].
- 322 • To reduce the potential effect of ascertainment bias on SNP array data and of cytosine
323 deamination on transition SNPs, we also ascertained 1,797,398 transversion SNPs with a
324 minor allele frequency of at least 10% (to avoid the effect of Eurasian admixture into

Yorubans) in Yorubans of the 1000 genomes project [27]. Those SNPs were extracted using vcftools [63].

These data sets were merged with ancient individuals of less than 15x genome coverage using the following approach: for each SNP site, a random read covering that site with minimum mapping quality 30 was drawn (using samtools 0.1.19 mpileup [64]) and its allele was assumed to be homozygous in the ancient individual. Transition sites were coded as missing data for individuals that were not UDG treated and SNPs showing additional alleles or indels in the ancient individuals were excluded from the data.

Six high coverage ancient individuals (SF12, NE1 [24], Kotias [32], Loschbour [16], Stuttgart [16], Ust-Ishim [36]) used in this study were treated differently as we generated diploid genotype calls for them. First, the base qualities of all Ts in the first five base pairs of each read as well as all As in the last five base pairs were set to 2. We then used Picard [65] to add read groups to the files. Indel realignment was conducted with GATK 3.5.0 [66] using indels identified in phase 1 of the 1000 genomes project as reference [27]. Finally, GATK's UnifiedGenotyper was used to call diploid genotypes with the parameters -stand_call_conf 50.0, -stand_emit_conf 50.0, -mbq 30, -contamination 0.02 and --output_mode EMIT_ALL_SITES using dbSNP version 142 as known SNPs. SNP sites from the reference data sets were extracted from the VCF files using vcftools [63] if they were not marked as low quality calls. Plink 1.9 [67,68] was used to merge the different data sets.

347 We performed principal component analysis (PCA) to characterize the genetic affinities of the
 348 ancient Scandinavian genomes to previously published ancient and modern genetic variation.
 349 PCA was conducted on 42 present-day west Eurasian populations from the Human Origins
 350 dataset [16,37], using *smartpca* [69] with numoutlieriter: 0 and lsqproject: YES options. A total
 351 of 59 ancient genomes (52 previously published and 7 reported here) (Table S6.1) were projected
 352 into the reference PCA space, computed from the genotype of modern individuals. For all
 353 individuals, a single allele was selected randomly making the data set fully homozygous. The
 354 result was plotted using the *ploteig* program of the EIGENSOFT [69] using with the $-x$ and $-k$
 355 options.

356

357 *D and f statistics*: The qpDstat program of ADMIXTOOLS was used to calculate *D*-statistics to
 358 test deviations from a tree-like population topology of the shape $((A,B);(X,Y))$ [37]. Standard
 359 errors were calculated using a block jackknife of 0.5 Mbp. The tree topologies are balanced at
 360 zero, indicating no recent interactions between the test populations. Significant deviations from
 361 zero indicate a deviation from the proposed tree topology depending on the value. Positive values
 362 indicate an excess of shared alleles between A and X or B and Y while negative values indicate
 363 more shared alleles between B and X or A and Y. Using an outgroup as population A limits the
 364 test results to depend on the recent relationships between B and Y (if positive) or B and X (if
 365 negative). Here we used high-coverage Mota [35], Yoruba [27] and Chimp genome as (A)
 366 outgroups. The software popstats [70] was used to calculate *f4* statistics, in order to estimate
 367 shared drift between groups. Standard errors and Z scores for *f4* statistics were estimated using a
 368 weighted block jackknife (Fig. 1C).

369

370 *Model-based clustering*: A model-based clustering algorithm, implemented in the ADMIXTURE
 371 software [71], was used to estimate ancestry components and to cluster individuals.
 372 ADMIXTURE was conducted on the Human Origins data set [16,37], which was merged with
 373 the ancient individuals as described above. Data was pseudo-haploidized by randomly selecting
 374 one allele at each heterozygous site of present-day individuals. Finally, the dataset was filtered
 375 for linkage disequilibrium using PLINK [67,68] with parameters (--indep-pairwise 200 25 0.4),
 376 this retained 289,504 SNPs. ADMIXTURE was run in 50 replicates with different random seeds
 377 for ancestral clusters from K=2 to K=20. Common signals between independent runs for each K
 378 were identified using the LargeKGreedy algorithm of CLUMPP [72]. Clustering was visualized
 379 using rworldmap, ggplot2, SDMTtools and RColorBrewer packages of GNU R version 3.3.0.
 380 Starting from K=3, when the modern samples split up into an African and Eastern and Western
 381 Eurasian clusters, the Mesolithic Scandinavians from Norway show slightly higher proportions of
 382 the Eastern cluster than Swedish Mesolithic individuals. This pattern continues to develop across
 383 higher values of K and it is consistent with the higher Eastern affinities of the Norwegian samples
 384 seen in the PCA and D/f₄ statistics. The results for all Ks are shown in S1 Fig..

385 In addition to ADMIXTURE, we assessed the admixture patterns in Mesolithic Scandinavians
 386 using a set of methods implemented in ADMIXTOOLS [37], qpWave [73] and qpAdm [16,17].
 387 Both methods are based on f₄ statistics, which relate a set of test populations to a set of outgroups
 388 in different distances from the potential source populations. We used the following set of
 389 outgroup populations from the Human Origins data set: Ami_Coriell, Biaka, Bougainville,
 390 Chukchi, Eskimo_Naukan, Han, Karitiana, Kharia, Onge. We first used qpWave to test the
 391 number of source populations for Mesolithic West Eurasians (WHG). qpWave calculates a set of
 392 statistics $X(u,v) = f_4(u_0, u; v_0, v)$ where u_0 and v_0 are populations from the sets of test

393 populations L and outgroups R, respectively. To avoid having more test populations than
 394 outgroups, we built four groups consisting of (a) genetically western and central hunter-gatherers
 395 (Bichon, Loschbour, KO1, LaBrana), (b) Eastern hunter-gatherers (UzOO74/I0061,
 396 SVP44/I0124, UzOO40/I0211) (c) Norwegian hunter-gathers (Hum1, Hum2, Steigen) and (d)
 397 Swedish hunter-gatherers (individuals from Motala and Mesolithic Gotland). qpWave tests the
 398 rank of the matrix of all $X(u,v)$ statistics. If the matrix has rank m , the test populations can be
 399 assumed to be related to at least $m+1$ “waves” of ancestry, which are differently related to the
 400 outgroups. A rank of 0 is rejected in our case ($p=3.13e-81$) while a rank of 1 is consistent with the
 401 data ($p=0.699$). Haak et al 2015 already showed, using the same approach, that WHG and EHG
 402 descend from at least two sources (confirmed with our data as rank 0 is rejected with $p=1.66e-86$,
 403 while rank 1 is consistent with the data) and adding individuals from Motala does not change
 404 these observations. Therefore, we conclude that European Mesolithic populations, including
 405 Swedish and Norwegian Mesolithic individuals, have at least two source populations.

406 We then used qpAdm to model Mesolithic Scandinavian individuals as a 2-way admixture of
 407 WHG and EHG. qpAdm was run separately for each Scandinavian individual x , setting $T=x$ as
 408 target and $S=\{EHG, WHG\}$ as sources. The general approach of qpAdm is related to qpWave:
 409 target and source are used as L (with T being the base population) and f_4 statistics with outgroups
 410 from R (same as above) are calculated. The rank of the resulting matrix is then set to the number
 411 of sources minus one, which allows to estimate the admixture contributions from each
 412 populations in S to T. The results are shown in Fig. 1.

413

414 *Runs of homozygosity*: Heterozygosity is a measurement for general population diversity and its
 415 effective population size. Analyzing the extent of homozygous segments across the genome can
 416 also give us a temporal perspective on the effective population sizes. Many short segments of
 417 homozygous SNPs can be connected to historically small population sizes while an excess of
 418 long runs of homozygosity suggests recent inbreeding. We restricted this analysis to the six high
 419 coverage individuals (SF12, NE1, Kotias, Loschbour, Stuttgart, Ust-Ishim) for which we obtained
 420 diploid genotype calls and we compared them to modern individuals from the 1000 genomes
 421 project. The length and number of runs of homozygosity were estimated using Plink 1.9 [67,68]
 422 and the parameters --homozyg-density 50, --homozyg-gap 100, --homozyg-kb 500, --homozyg-
 423 snp 100, --homozyg-window-het 1, --homozyg-window-snp 100, --homozyg-window-threshold
 424 0.05 and --homozyg-window-missing 20. The results are shown in Fig. 2A.

425

426 *Linkage disequilibrium*: Similar to runs of homozygosity, the decay of linkage disequilibrium
 427 (LD) harbors information on the demographic history of a population. Long distance LD can be
 428 caused by a low effective population size and past bottlenecks. Calculating LD for ancient DNA
 429 data is challenging as the low amounts of authentic DNA usually just yields haploid allele calls
 430 with unknown phase. In order to estimate LD decay for ancient populations we first combine two
 431 haploid ancient individuals to a pseudo-diploid individual (similar to the approach chosen for
 432 conditional nucleotide diversity, S7 Text). Next, we bin SNP pairs by distance (bin size 5kb) and
 433 then calculate the covariance of derived allele frequencies (0, 0.5 or 1.0) for each bin. This way,
 434 we do not need phase information to calculate LD decay as we do not consider multilocus
 435 haplotypes, which is similar to the approach taken by ROLLOFF[37,74] and ALDER [75] to date
 436 admixture events based on admixture LD decay. For Fig. 2B, we used two modern 1000 genomes

437 populations to scale the LD per bin. The LD between two randomly chosen PEL (Peruvian)
 438 individuals was set to 1 and the LD between two randomly chosen TSI (Tuscan) individuals was
 439 set to 0. This approach is used to obtain a relative scale for the ancient populations and we
 440 caution against a direct interpretation of the differences to modern populations as technical
 441 differences in the modern data (e.g. SNP calling or imputation) may have substantial effects.

442

443 *Effective population size:* We are using MSMC's implementation of PSMC' [39] to infer effective
 444 population sizes over time from single high coverage genomes. We restrict this analysis to UDG-
 445 treated individuals (SF12, Loschbour, Stuttgart, Ust-Ishim) as post-mortem damage would cause
 446 an excess of false heterozygous transition sites. Input files were prepared using scripts provided
 447 with the release of MSMC (<https://github.com/stschiiff/msmc-tools>) and MSMC was run with the
 448 non-default parameters --fixedRecombination and -r 0.88 in order to set the ratio of
 449 recombination to mutation rate to a realistic level for humans. We also estimate effective
 450 population size for six high-coverage modern genomes [76] (Fig. 2C). We plot the effective
 451 population size assuming a mutation rate of 1.25×10^{-8} and a generation time of 30 years. The
 452 curves for ancient individuals were shifted based on their average C14 date.

453

454 ***Detecting adaptation to high-latitude environments***

455 We scanned the genomes for SNPs with similar allele frequencies in Mesolithic and modern-day
 456 northern Europeans, and contrast it to a modern-day population from southern latitudes. Pooling
 457 all Mesolithic Scandinavians together, we obtain an allele frequency estimate for Scandinavian
 458 hunter-gatherers (SHG) which is compared to modern-day Finnish individuals (FIN) and Tuscan

459 individuals (TSI) from the 1000 genomes project [27]. We use the Finnish population as
 460 representatives of modern-day northern Europeans (this sample contains the largest number of
 461 sequenced genomes from a northern European population). Tuscans are used as an alternative
 462 population, who also traces some ancestry to Mesolithic populations, but who do not trace their
 463 ancestry to groups that lived at northern latitudes in the last 7-9,000 years. Our approach is
 464 similar to PBS [77] and inspired by DAnc [40], for each SNP, we calculate the statistic D_{sel}
 465 comparing the allele frequencies between an ancestral and two modern populations:

466

$$467 D_{sel} = |DAF_{SHG} - DAF_{TSI}| - |DAF_{SHG} - DAF_{FIN}|$$

468

469 This scan was performed on all transversion SNPs extracted from the 1000 genomes data. Only
 470 sites with a high confidence ancestral allele in the human ancestor (as used by the 1000 genomes
 471 project [27]) and with coverage for at least six ancient Scandinavians were included in the com-
 472 putation. More information can be found in S10 Text.

473

474

475 **Acknowledgements**

476 We thank Rachel Howcroft, and Nicci Arosén for help with isotope laboratory work and Heike
 477 Siegmund at the Stable Isotope Laboratory, Stockholm University, Lena Idestrom at Gotlands
 478 museum and Sabine Sten at Uppsala University Campus Gotland in assisting in sampling the
 479 Stora Bjers material, Leena Drenzel at The Swedish History Museum for assistance with the

480 Stora Förvar material, and the Norwegian Maritime Museum for excavating Hummervikholmen.
 481 MS and PC thank the participants who volunteered for face reconstruction methods development.
 482 This project was supported by grants from Riksbankens Jubileumsfond (to AG, MJ, and JS), Knut
 483 and Alice Wallenberg foundation (to MJ, JS, AG), the Swedish Research council, no. 2013-1905
 484 (to AG, MJ, and JS) and no. 421-2013-730 (to JA and JS), an European Research Council Start-
 485 ing Grant (to MJ), a Wenner-Gren foundations postdoctoral fellowship (to TG), and Berit Wallen-
 486 berg foundation (to MF). Sequencing was performed at the National Genomics Infrastructure
 487 (NGI) Uppsala and computations were performed at Uppsala Multidisciplinary Center for Ad-
 488 vanced Computational Science (UPPMAX).

Figure legends

491

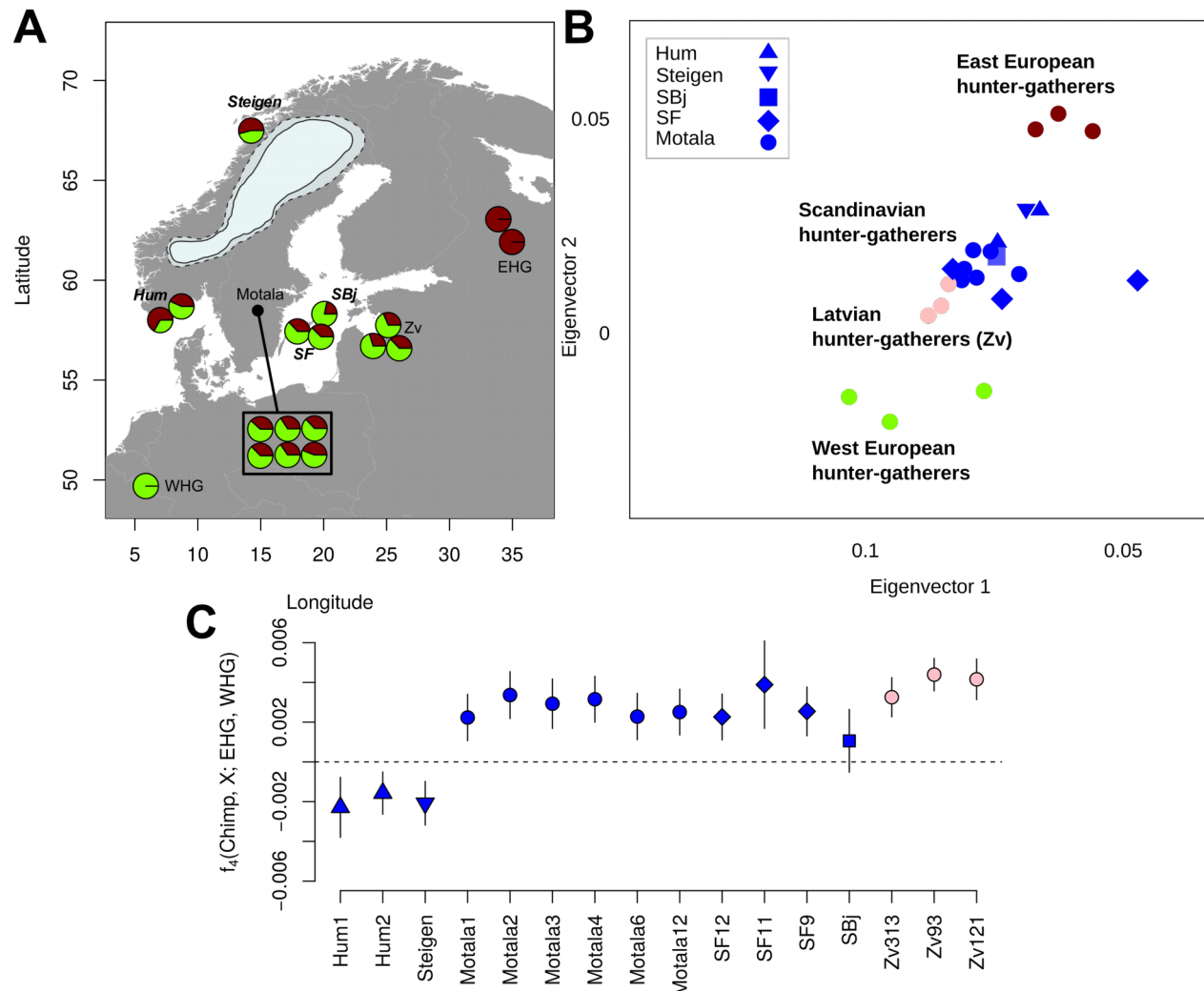


Fig. 1: Mesolithic samples and their genetic affinities – (A) Map of the Mesolithic European samples used in this study. The pie charts show the model-based [16,17] estimates of genetic ancestry for each SHG individual. The map also displays the ice sheet covering Scandinavia 10,000 BP (most credible (solid line) and maximum extend (dashed line) following [10]). Newly sequenced sites are shown in bold and italics, SF11 is excluded from this map due to its low coverage (0.1x). Additional European EHG and WHG individuals used in this study derive from sites outside this map. (B) Magnified section of genetic similarity among ancient and modern-day individuals using PCA featuring only the Mesolithic European samples (see S6 Text for the full plot). (C) Allele sharing between the SHGs, Latvian Mesolithic hunter-gatherers [33] and EHG vs WHGs measured by $f_4(\text{Chimpanzee}, \text{SHG}; \text{EHG}, \text{WHG})$ calculated for the captured SNPs for the EHG [18]. Error bars show two block-jackknife standard errors.

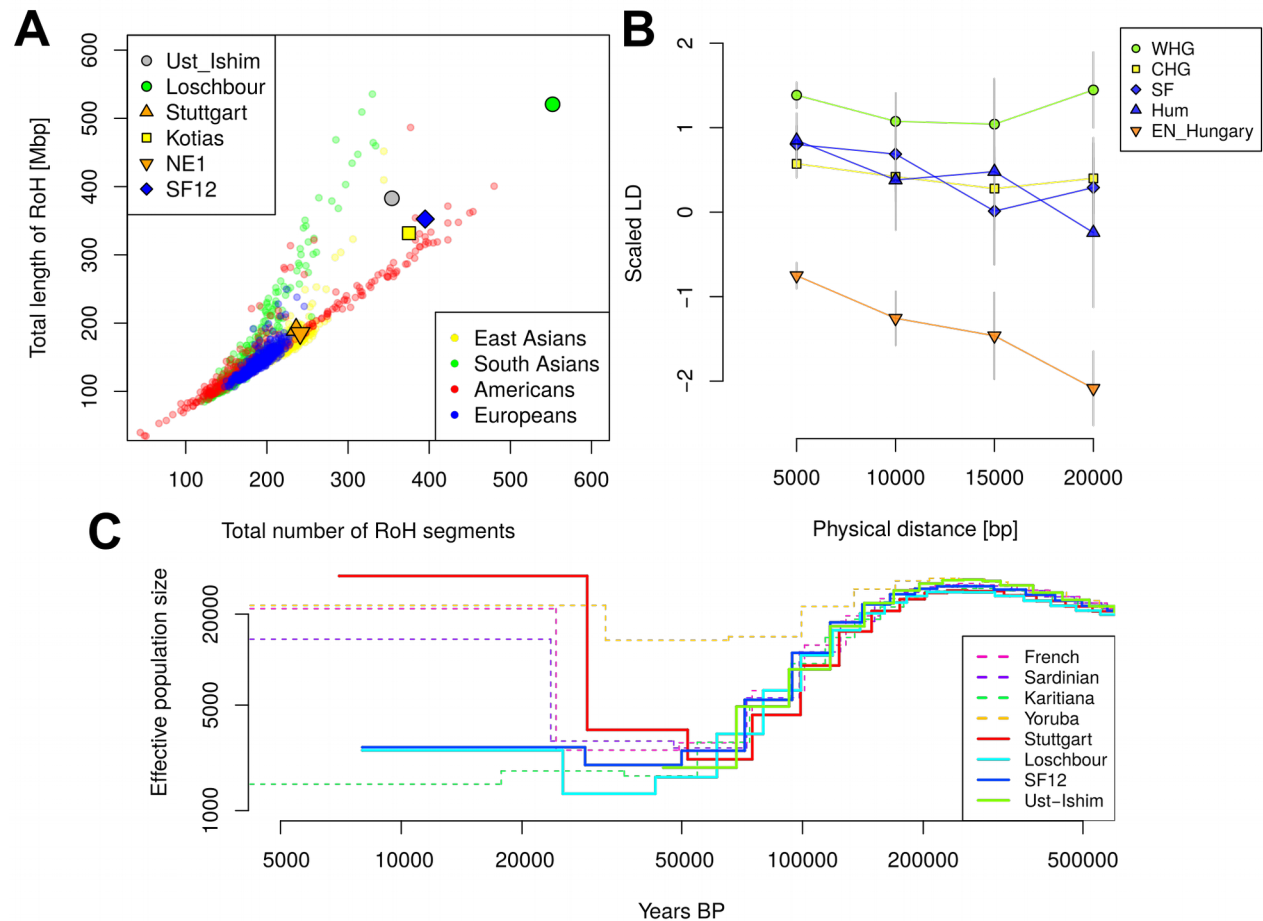


Fig. 2: Genetic diversity in prehistoric Europe – (A) Runs of Homozygosity (RoH) for the six prehistoric humans that have been sequenced to >20x genome coverage, (Kotias is a hunter-gatherer from the Caucasus region [32], NE1 is an early Neolithic individual from modern-day Hungary [24], the other individuals are described in the text), compared to all modern-day non-African individuals from the 1000 genomes project [27]. (B) Linkage disequilibrium (LD) decay for five prehistoric populations each represented by two individuals (eastern SHGs: SF (SF9 and SF12), western SHGs: Hum (Hum1 and Hum2), Caucasus hunter-gatherers [32]: CHG (Kotias and Satsurbliia), WHGs [16,32] (Loschbour and Bichon), and early Neolithic Hungarians [24]: EN_Hungary (NE1 and NE6). LD was scaled in each distance bin by using the LD for two modern populations [27] as 1 (modern-day Tuscan, TSI) and as 0 (modern-day Peruvians, PEL). LD was calculated from the covariance of derived allele frequencies of two haploid individuals per population (S7 Text). Error bars show two standard errors estimate during 100 bootstraps across SNP pairs. (C) Effective population size over time as inferred by MSMC' [39] for four prehistoric humans with high genome coverage. The dashed lines show the effective population sizes for modern-day populations. All curves for prehistoric individuals were shifted along the X axis according to their radiocarbon date.

521

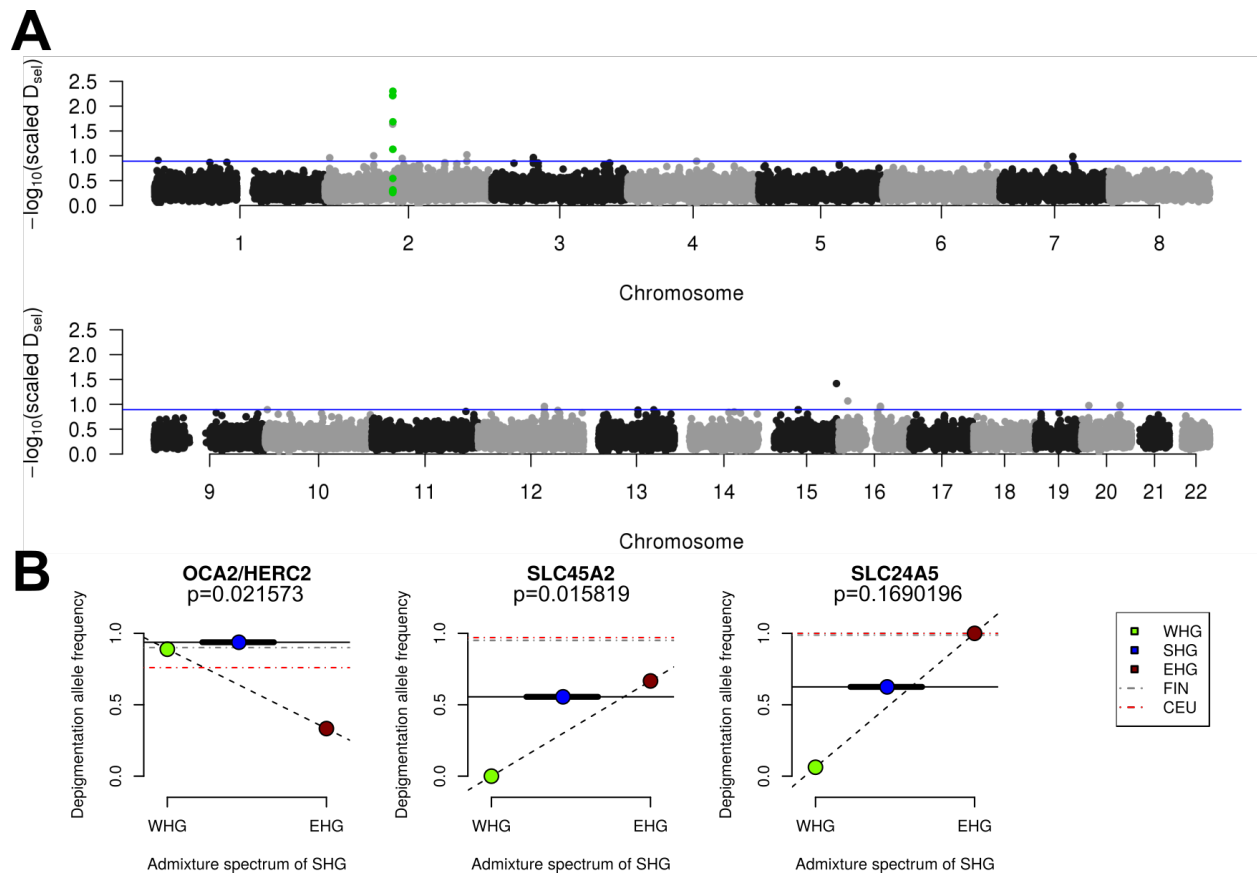


Fig. 3: Adaptation to high-latitude climates – (A) Manhattan plot of similarity between Mesolithic allele-frequency and modern-day Finnish (FIN) allele-frequency in contrast to difference to (TSI) allele-frequency using the statistic D_{sel} . The green-highlighted SNPs are all located in the *TMEM131* gene. The horizontal blue line depicts the top 0.01% D_{sel} SNPs across the genome. (B) Derived allele frequencies for three pigmentation associated SNPs (*SLC24A5*, *SLC45A2*, associated with skin pigmentation and *OCA2/HERC2* associated with eye pigmentation). The dashed line connecting EHG and WHG represents potential allele frequencies if SHG were a linear combination of admixture between EHG and WHG. The solid horizontal line represents the derived allele frequency in SHG. The blue symbols representing SHGs were set on the average genome-wide WHG/EHG mixture proportion (on x-axis) across all SHGs, the thick black line represents the minimum and maximum admixture proportions across all SHGs. Dashed horizontal lines represent modern European populations (CEU=Utah residents with Central European ancestry). The p-values were estimated from simulations of SHG allele frequencies based on their genome-wide ancestry proportions (S10 Text).

537

538 References

1. Andersen B, Borns HW. The ice age world: an introduction to quaternary history and research with emphasis on North America and Northern Europe during the last 2.5 million years. Oslo [u.a.: Scandinavian Univ. Press; 1994.
2. Parducci L, Jorgensen T, Tollefsrud MM, Elverland E, Alm T, Fontana SL, et al. Glacial Survival of Boreal Trees in Northern Scandinavia. *Science*. 2012;335: 1083–1086. doi:10.1126/science.1216043
3. François O, Blum MGB, Jakobsson M, Rosenberg NA. Demographic History of European Populations of *Arabidopsis thaliana*. *PLOS Genetics*. 2008;4: e1000075. doi:10.1371/journal.pgen.1000075
4. Hewitt G. The genetic legacy of the Quaternary ice ages. *Nature*. 2000;405: 907–913. doi:10.1038/35016000
5. Xenikoudakis G, Ersmark E, Tison J-L, Waits L, Kindberg J, Swenson JE, et al. Consequences of a demographic bottleneck on genetic structure and variation in the Scandinavian brown bear. *Mol Ecol*. 2015;24: 3441–3454. doi:10.1111/mec.13239
6. Riede F. The resettlement of Northern Europe. In: Cummings V, Jordan P, Zvelebil M, editors. *The Oxford Handbook of the Archaeology and Anthropology of Hunter-Gatherers*. Oxford University Press; 2014.
7. Kankaanpää J, Rankama T. Fast or slow pioneers? A view from northern Lapland. In: Riede F, Tallavaara M, editors. *Lateglacial and Postglacial Pioneers in Northern Europe*, BAR International Series. Oxford: Oxford Archaeopress; 2014. pp. 147–154.
8. Breivik HM. Palaeo-oceanographic development and human adaptive strategies in the Pleistocene–Holocene transition: A study from the Norwegian coast. *The Holocene*. 2014;24: 1478–1490.
9. Stroeve AP, Hättestrand C, Kleman J, Heyman J, Fabel D, Fredin O, et al. Deglaciation of Fennoscandia. *Quaternary Science Reviews*. 2016;147: 91–121.
10. Hughes AL, Gyllencreutz R, Lohne ØS, Mangerud J, Svendsen JJ. The last Eurasian ice sheets—a chronological database and time-slice reconstruction, DATED-1. *Boreas*. 2016;45: 1–45.
11. Bjerck HB, Breivik HM, Piana EL, Zangrando AF. Exploring the role of pinnipeds in the human colonization of the seascapes of Patagonia and Scandinavia. In: Bjerck HB, Breivik HM, Fretheim SE, Piana EL, Skar B, Tivoli AM, et al., editors. *Equinox* Sheffield; 2016. pp. 53–74.
12. Sørensen M, Rankama T, Kankaanpää J, Knutsson K, Knutsson H, Melvold S, et al. The First Eastern Migrations of People and Knowledge into Scandinavia: Evidence from Studies of Mesolithic Technology, 9th–8th Millennium BC. *Norwegian Archaeological Review*. 2013;46: 19–56. doi:10.1080/00293652.2013.770416
13. Knutsson H, Knutsson K, Molin F, Zetterlund P. From flint to quartz: Organization of lithic technology in relation to raw material availability during the pioneer process of Scandinavia. *Quaternary International*. 2016;424: 32–57. doi:10.1016/j.quaint.2015.10.062

14. Skoglund P, Malmstrom H, Raghavan M, Stora J, Hall P, Willerslev E, et al. Origins and Genetic Legacy of Neolithic Farmers and Hunter-Gatherers in Europe. *Science*. 2012;336: 466–469. doi:10.1126/science.1216304
15. Skoglund P, Malmstrom H, Omrak A, Raghavan M, Valdiosera C, Gunther T, et al. Genomic Diversity and Admixture Differs for Stone-Age Scandinavian Foragers and Farmers. *Science*. 2014;344: 747–750. doi:10.1126/science.1253448
16. Lazaridis I, Patterson N, Mittnik A, Renaud G, Mallick S, Kirsanow K, et al. Ancient human genomes suggest three ancestral populations for present-day Europeans. *Nature*. 2014;513: 409–413. doi:10.1038/nature13673
17. Haak W, Lazaridis I, Patterson N, Rohland N, Mallick S, Llamas B, et al. Massive migration from the steppe was a source for Indo-European languages in Europe. *Nature*. 2015;522: 207–211. doi:10.1038/nature14317
18. Mathieson I, Lazaridis I, Rohland N, Mallick S, Patterson N, Roodenberg SA, et al. Genome-wide patterns of selection in 230 ancient Eurasians. *Nature*. 2015;528: 499–503. doi:10.1038/nature16152
19. Olalde I, Allentoft ME, Sánchez-Quinto F, Santpere G, Chiang CWK, DeGiorgio M, et al. Derived immune and ancestral pigmentation alleles in a 7,000-year-old Mesolithic European. *Nature*. 2014;507: 225–228. doi:10.1038/nature12960
20. Raghavan M, Skoglund P, Graf KE, Metspalu M, Albrechtsen A, Moltke I, et al. Upper Palaeolithic Siberian genome reveals dual ancestry of Native Americans. *Nature*. 2013;505: 87–91. doi:10.1038/nature12736
21. Fu Q, Posth C, Hajdinjak M, Petr M, Mallick S, Fernandes D, et al. The genetic history of Ice Age Europe. *Nature*. 2016;534: 200–5. doi:10.1038/nature17993
22. Cummings V, Jordan P, Zvelebil M, editors. *The Oxford Handbook of the Archaeology and Anthropology of Hunter-Gatherers*. Oxford University Press; 2014. doi:10.1093/oxfordhb/9780199551224.001.0001
23. Allentoft ME, Sikora M, Sjögren K-G, Rasmussen S, Rasmussen M, Stenderup J, et al. Population genomics of Bronze Age Eurasia. *Nature*. 2015;522: 167–172. doi:10.1038/nature14507
24. Gamba C, Jones ER, Teasdale MD, McLaughlin RL, Gonzalez-Fortes G, Mattiangeli V, et al. Genome flux and stasis in a five millennium transect of European prehistory. *Nature Communications*. 2014;5: 5257. doi:10.1038/ncomms6257
25. Sjögren K-G, Ahlström T. Early Mesolithic burials from Bohuslän, western Sweden. *Mesolithic burials – Rites, symbols and social organisation of early postglacial communities*. Beier & Beran; 2017.
26. Briggs AW, Stenzel U, Meyer M, Krause J, Kircher M, Pääbo S. Removal of deaminated cytosines and detection of in vivo methylation in ancient DNA. *Nucleic Acids Res*. 2010;38: e87–e87. doi:10.1093/nar/gkp1163
27. Auton A, Abecasis GR, Altshuler DM, Durbin RM, Abecasis GR, Bentley DR, et al. A global reference for human genetic variation. *Nature*. 2015;526: 68–74. doi:10.1038/nature15393

28. Cingolani P, Platts A, Wang LL, Coon M, Nguyen T, Wang L, et al. A program for annotating and predicting the effects of single nucleotide polymorphisms, SnpEff: SNPs in the genome of *Drosophila melanogaster* strain w¹¹¹⁸; iso-2; iso-3. *Fly*. 2012;6: 80–92. doi:10.4161/fly.19695
29. Nixon B, Bromfield E, Dun M, Redgrove K, McLaughlin E, Aitken Rj. The role of the molecular chaperone heat shock protein A2 (HSPA2) in regulating human sperm-egg recognition. *Asian Journal of Andrology*. 2015;17: 568. doi:10.4103/1008-682X.151395
30. Claes P, Liberton DK, Daniels K, Rosana KM, Quillen EE, Pearson LN, et al. Modeling 3D Facial Shape from DNA. Luquetti D, editor. *PLoS Genetics*. 2014;10: e1004224. doi:10.1371/journal.pgen.1004224
31. Claes P, Hill H, Shriver MD. Toward DNA-based facial composites: preliminary results and validation. *Forensic Science International: Genetics*. 2014;13: 208–216.
32. Jones ER, Gonzalez-Fortes G, Connell S, Siska V, Eriksson A, Martiniano R, et al. Upper Palaeolithic genomes reveal deep roots of modern Eurasians. *Nature communications*. 2015;6: 8912. doi:10.1038/ncomms9912
33. Jones ER, Zarina G, Moiseyev V, Lightfoot E, Nigst PR, Manica A, et al. The Neolithic Transition in the Baltic Was Not Driven by Admixture with Early European Farmers. *Curr Biol*. 2017;27: 576–582. doi:10.1016/j.cub.2016.12.060
34. Seguin-Orlando A, Korneliussen TS, Sikora M, Malaspinas A-S, Manica A, Moltke I, et al. Genomic structure in Europeans dating back at least 36,200 years. *Science*. 2014;346: 1113–1118. doi:10.1126/science.aaa0114
35. Llorente MG, Jones ER, Eriksson A, Siska V, Arthur KW, Arthur JW, et al. Ancient Ethiopian genome reveals extensive Eurasian admixture throughout the African continent. *Science*. 2015;350: 820–2. doi:10.1126/science.aad2879
36. Fu Q, Li H, Moorjani P, Jay F, Slepchenko SM, Bondarev AA, et al. Genome sequence of a 45,000-year-old modern human from western Siberia. *Nature*. 2014;514: 445–449. doi:10.1038/nature13810
37. Patterson N, Moorjani P, Luo Y, Mallick S, Rohland N, Zhan Y, et al. Ancient Admixture in Human History. *Genetics*. 2012;192: 1065–1093. doi:10.1534/genetics.112.145037
38. Günther T, Jakobsson M. Genes mirror migrations and cultures in prehistoric Europe-a population genomic perspective. *Curr Opin Genet Dev*. 2016;41: 115–123. doi:10.1016/j.gde.2016.09.004
39. Schiffels S, Durbin R. Inferring human population size and separation history from multiple genome sequences. *Nature genetics*. 2014;46: 919–25. doi:10.1038/ng.3015
40. Key FM, Fu Q, Romagné F, Lachmann M, Andrés AM. Human adaptation and population differentiation in the light of ancient genomes. *Nature Communications*. 2016;7: 10775. doi:10.1038/ncomms10775
41. Vasan RS, Larson MG, Aragam J, Wang TJ, Mitchell GF, Kathiresan S, et al. Genome-wide association of echocardiographic dimensions, brachial artery endothelial function and treadmill exercise responses in the Framingham Heart Study. *BMC Medical Genetics*. 2007;8: S2. doi:10.1186/1471-2350-8-S1-S2

42. Makinen TM. Different types of cold adaptation in humans. *Frontiers in bioscience*. 2010;2: 1047–1067. doi:10.2741/S117
43. Fan S, Hansen MEB, Lo Y, Tishkoff SA. Going global by adapting local: A review of recent human adaptation. *Science*. 2016;354: 54–59. doi:10.1126/science.aaf5098
44. Donnelly MP, Paschou P, Grigorenko E, Gurwitz D, Barta C, Lu RB, et al. A global view of the OCA2-HERC2 region and pigmentation. *Human Genetics*. 2012;131: 683–696. doi:10.1007/s00439-011-1110-x
45. Jablonski NG, Chaplin G. The colours of humanity: the evolution of pigmentation in the human lineage. *Philosophical Transactions of the Royal Society B: Biological Sciences*. 2017;372: 20160349. doi:10.1098/rstb.2016.0349
46. Nielsen R, Akey JM, Jakobsson M, Pritchard JK, Tishkoff S, Willerslev E. Tracing the peopling of the world through genomics. *Nature*. 2017;541: 302–310. doi:10.1038/nature21347
47. Hofmanová Z, Kreutzer S, Hellenthal G, Sell C, Diekmann Y, Díez-del-Molino D, et al. Early farmers from across Europe directly descended from Neolithic Aegeans. *PNAS*. 2016; 201523951. doi:10.1073/pnas.1523951113
48. Cassidy LM, Martiniano R, Murphy EM, Teasdale MD, Mallory J, Hartwell B, et al. Neolithic and Bronze Age migration to Ireland and establishment of the insular Atlantic genome. *Proceedings of the National Academy of Sciences*. 2015; 1–6. doi:10.1073/pnas.1518445113
49. Günther T, Valdiosera C, Malmström H, Ureña I, Rodriguez-Varela R, Sverrisdóttir ÓO, et al. Ancient genomes link early farmers from Atapuerca in Spain to modern-day Basques. *Proc Natl Acad Sci USA*. 2015;112: 11917–11922. doi:10.1073/pnas.1509851112
50. Olalde I, Schroeder H, Sandoval-Velasco M, Vinner L, Lobón I, Ramirez O, et al. A common genetic origin for early farmers from mediterranean cardial and central european LBK cultures. *Molecular Biology and Evolution*. 2015;32: 3132–3142. doi:10.1093/molbev/msv181
51. Yang DY, Eng B, Wayne JS, Dudar JC, Saunders SR. Technical note: improved DNA extraction from ancient bones using silica-based spin columns. *Am J Phys Anthropol*. 1998;105: 539–543. doi:10.1002/(SICI)1096-8644(199804)105:4<539::AID-AJPA10>3.0.CO;2-1
52. Malmström H, Svensson EM, Gilbert MTP, Willerslev E, Götherström A, Holmlund G. More on contamination: The use of asymmetric molecular behavior to identify authentic ancient human DNA. *Molecular Biology and Evolution*. 2007;24: 998–1004. doi:10.1093/molbev/msm015
53. Dabney J, Knapp M, Glocke I, Gansauge M-T, Weihmann A, Nickel B, et al. Complete mitochondrial genome sequence of a Middle Pleistocene cave bear reconstructed from ultrashort DNA fragments. *Proc Natl Acad Sci USA*. 2013;110: 15758–15763. doi:10.1073/pnas.1314445110
54. Meyer M, Kircher M. Illumina Sequencing Library Preparation for Highly Multiplexed Target Capture and Sequencing. *Cold Spring Harbor Protocols*. 2010;2010: pdb.prot5448-pdb.prot5448. doi:10.1101/pdb.prot5448
55. Briggs AW, Heyn P. Preparation of next-generation sequencing libraries from damaged DNA. *Methods in Molecular Biology*. 2012;840: 143–154. doi:10.1007/978-1-61779-516-9_18

56. Kircher M. Analysis of high-throughput ancient DNA sequencing data. *Methods Mol Biol.* 2012;840: 197–228. doi:10.1007/978-1-61779-516-9_23
57. Li H, Durbin R. Fast and accurate short read alignment with Burrows-Wheeler transform. *Bioinformatics.* 2009;25: 1754–1760. doi:10.1093/bioinformatics/btp324
58. Kuhn JMM, Jakobsson M, Günther T. Estimating genetic kin relationships in prehistoric populations. *bioRxiv.* 2017; 100297.
59. Green RE, Malaspina A-S, Krause J, Briggs AW, Johnson PLF, Uhler C, et al. A Complete Neandertal Mitochondrial Genome Sequence Determined by High-Throughput Sequencing. *Cell.* 2008;134: 416–426. doi:10.1016/j.cell.2008.06.021
60. Rasmussen M, Guo X, Wang Y, Lohmueller KE, Rasmussen S, Albrechtsen A, et al. An Aboriginal Australian genome reveals separate human dispersals into Asia. *Science.* 2011;334: 94–98. doi:10.1126/science.1211177
61. Korneliussen TS, Albrechtsen A, Nielsen R. ANGSD: Analysis of Next Generation Sequencing Data. *BMC Bioinformatics.* 2014;15: 356. doi:10.1186/s12859-014-0356-4
62. Jun G, Flickinger M, Hetrick KN, Romm JM, Doheny KF, Abecasis GR, et al. Detecting and estimating contamination of human DNA samples in sequencing and array-based genotype data. *American Journal of Human Genetics.* 2012;91: 839–848. doi:10.1016/j.ajhg.2012.09.004
63. Danecek P, Auton A, Abecasis G, Albers CA, Banks E, DePristo MA, et al. The variant call format and VCFtools. *Bioinformatics.* 2011;27: 2156–2158. doi:10.1093/bioinformatics/btr330
64. Li H, Handsaker B, Wysoker A, Fennell T, Ruan J, Homer N, et al. The Sequence Alignment/Map format and SAMtools. *Bioinformatics.* 2009;25: 2078–2079. doi:10.1093/bioinformatics/btp352
65. Broad Institute. Picard tools. <https://broadinstitute.github.io/picard/>. 2016; Available: <http://broadinstitute.github.io/picard/>
66. Schmidt S. (GATK) The Genome Analysis Toolkit: A MapReduce framework for analyzing next-generation DNA sequencing data. *Proceedings of the International Conference on Intellectual Capital, Knowledge Management & Organizational Learning.* 2009;20: 254–260. doi:10.1101/gr.107524.110.20
67. Purcell S, Neale B, Todd-Brown K, Thomas L, Ferreira MAR, Bender D, et al. PLINK: a tool set for whole-genome association and population-based linkage analyses. *Am J Hum Genet.* 2007;81: 559–575. doi:10.1086/519795
68. Chang CC, Chow CC, Tellier LC, Vattikuti S, Purcell SM, Lee JJ. Second-generation PLINK: rising to the challenge of larger and richer datasets. *Gigascience.* 2015;4: 7.
69. Patterson N, Price AL, Reich D. Population Structure and Eigenanalysis. *PLoS Genetics.* 2006;2: e190. doi:10.1371/journal.pgen.0020190
70. Skoglund P, Mallick S, Bortolini MC, Chennagiri N, Hünemeier T, Petzl-Erler ML, et al. Genetic evidence for two founding populations of the Americas. *Nature.* 2015;525: 104–108.

71. Alexander DH, Novembre J, Lange K. Fast model-based estimation of ancestry in unrelated individuals. *Genome Res.* 2009;19: 1655–1664. doi:10.1101/gr.094052.109
72. Jakobsson M, Rosenberg NA. CLUMPP: a cluster matching and permutation program for dealing with label switching and multimodality in analysis of population structure. *Bioinformatics.* 2007;23: 1801–1806. doi:10.1093/bioinformatics/btm233
73. Reich D, Patterson N, Campbell D, Tandon A, Mazieres S, Ray N, et al. Reconstructing Native American population history. *Nature.* 2012;488: 370–374. doi:10.1038/nature11258
74. Moorjani P, Patterson N, Hirschhorn JN, Keinan A, Hao L, Atzmon G, et al. The history of african gene flow into Southern Europeans, Levantines, and Jews. *PLoS Genetics.* 2011;7. doi:10.1371/journal.pgen.1001373
75. Loh PR, Lipson M, Patterson N, Moorjani P, Pickrell JK, Reich D, et al. Inferring admixture histories of human populations using linkage disequilibrium. *Genetics.* 2013;193: 1233–1254. doi:10.1534/genetics.112.147330
76. Prüfer K, Racimo F, Patterson N, Jay F, Sankararaman S, Sawyer S, et al. The complete genome sequence of a Neanderthal from the Altai Mountains. *Nature.* 2014;505: 43–9. doi:10.1038/nature12886
77. Yi X, Liang Y, Huerta-Sanchez E, Jin X, Cuo ZXP, Pool JE, et al. Sequencing of 50 Human Exomes Reveals Adaptation to High Altitude. *Science.* 2010;329: 75–78. doi:10.1126/science.1190371